

Original Research Paper

# Green Synthesis of Silver Nanoparticles using Extract of *Disporopsis Longifolia* for Photocatalytic Degradation of Methylene Blue

<sup>3</sup>Khieu Thi Tam, <sup>1</sup>Dang Van Thanh, <sup>2</sup>Huu Tap Van, <sup>2</sup>Nguyen Thi Phuong Mai, <sup>3</sup>Cao Thanh Hai, <sup>3</sup>Tran Minh Phuong, <sup>1</sup>Nguyen Thi Xuan and <sup>4</sup>Van-Truong Nguyen

<sup>1</sup>TNU-University of Medicine and Pharmacy, Thai Nguyen City, Vietnam

<sup>2</sup>Faculty of Natural Resources and Environment, TNU-University of Sciences (TNUS), Tan Thinh Ward, Thai Nguyen City, Vietnam

<sup>3</sup>Faculty of Chemistry, TNU-University of Sciences, Tan Thinh Ward, Thai Nguyen City, Vietnam

<sup>4</sup>Department of Fundamental Sciences, Thai Nguyen University of Technology, Thai Nguyen City, Vietnam

## Article history

Received: 11-04-2022

Revised: 06-07-2022

Accepted: 01-10-2022

Corresponding Author:

Khieu Thi Tam

Faculty of Chemistry, TNU-University of Sciences, Tan Thinh ward, Thai Nguyen city, Vietnam

Email: tamkt@tnus.edu.vn

and

Van-Truong Nguyen

Department of Fundamental Sciences, Thai Nguyen University of Technology, Thai Nguyen City, Vietnam

Email: vtnguyen@tnut.edu.vn

**Abstract:** In this report, the silver Nanoparticles (AgNPs) were successfully synthesized in a simple one-pot method by the leaf and stem extract of *Disporopsis longifolia* as reducing, capping agents, and stabilizers for the first time. The optimal extract amount, AgNO<sub>3</sub> concentration, reaction temperature, and time for the AgNPs synthesis were identified using Ultraviolet-Visible (UV-Vis) spectroscopy. X-Ray Diffraction (XRD) and Scanning Electron Microscopy (SEM) were used to characterize the structure and morphology of the as-synthesized AgNPs. In addition, the characteristic vibration of the Ag-organic functional group was confirmed using Fourier Transform Infrared (FT-IR) spectroscopy. The as-synthesized AgNPs exhibited promising Methylene Blue (MB) photodegradation, resulting in approximately 100% removal after 240 min without any substantial silver leaching under the solar light. It is found that the AgNPs photocatalysis activity is improved by the synergy of the *Disporopsis longifolia* extract solution and can efficiently adapt to the photodegradation of organic dyes in industrial wastewater.

**Keywords:** Silver Nanoparticles, *Disporopsis Longifolia*, Photocatalysis, Methylene Blue

## Introduction

Nowadays, nanotechnology is playing an essential role in science and technology for optics, electronics, biomedical science, the chemical industry, catalysis, energy science, and photoelectrochemical applications due to their unique properties (Bera and Belhaj, 2016). Especially nanomaterials have been known as new materials that solve health problems and the environment (Mehdizadeh *et al.*, 2021). Nanoparticles have a high surface-to-volume ratio and extremely small size, resulting in changes in their physical and chemical properties compared to the majority of chemically identical materials (Bera and Belhaj, 2016; Hussain *et al.*, 2016; Gour and Jain, 2019; Salem and Fouda, 2021). Among many types of nanoparticles,

silver nanoparticles (AgNPs)-one metallic nanoparticle-have paid more attention owing to their unique optical, mechanical, thermal, and biological properties. Therefore, numerous approaches to synthesizing AgNPs such as Chemical Vapor Deposition (CVD) (Piszczyk and Radtke, 2018), impregnation (Mohammadalnejhad *et al.*, 2019), electrochemical (Kuntyi *et al.*, 2020), sol-gel (Maharjan, *et al.*, 2020) and microwave-assisted (Hong *et al.*, 2016). However, the toxic, costly, and/or non-environment factors are a great challenge for AgNP fabrication (Rafique *et al.*, 2017). *Green synthesis of AgNPs* is carried out by using microorganisms and plant extracts to address that issue (Mohammadi *et al.*, 2021; Mehdizadeh *et al.*, 2021). Plants are large factories with chemical constituents including

alkaloids, flavonoids, terpenoids, polyphenols, polysaccharides, and proteins which play a role in the reduction of metal ions to nanoparticles and stabilize formed metallic nanoparticles (Ishak *et al.*, 2019, Vanlalveni *et al.*, 2021). *Disporopsis longifolia* Crab, which belongs to *Disporopsis* (*D.*) genus, including seven known species, is mainly found in many countries such as Thailand, Laos, China, and Vietnam (Yang *et al.*, 2004; Nguyen *et al.*, 2006; Wang and Nie 2010). *D. longifolia* is a famous traditional Vietnamese medicine to treat many diseases including chronic cough, lack of blood, weakness, and irregular menstrual (Bich *et al.*, 2004; Chi, 2012). Besides, the chemical constituents of spirostan and furostan saponins in *D. longifolia* act as reducing agents and stabilizers for the biosynthesis of AgNPs. They exhibited strong anti-inflammatory activity for the inhibition of NO production in LPS-stimulated RAW 264.7 cells (Thu Ha *et al.*, 2021). However, there has been no research using the species in the *Disporopsis* genus for the synthesis of AgNPs.

Water pollution is a serious environmental problem around the world and one of the major pollutants is the organic dye wastewater with chemicals from the textile, plastic, and cosmetics industry that pose a significant environmental threat (Khatri *et al.*, 2015; Saini, 2017). Many hazardous organic dyes cannot be easily removed due to their complex nature and stability. Among them, methylene blue is one of the most important cationic dyes employed by textile industries for the dyeing process because its water solubility is high. MB causes serious health problems such as headache, dizziness, lack of blood, nausea, and mental confusion when in contact with it. Besides, it is harmful to aquatic and other organisms (Houas *et al.*, 2001; Gour and Jain, 2019). As a result, to treat industrial effluents and protect public health, efficient MB removal from wastewater is necessary (Tan *et al.*, 2016). There are both physical and chemical methods for removing MB. However, these methods are low adsorption capacity, biodegradability, high cost, and probable secondary pollution, which could produce concern in the environment and require the use of biodegradable materials, which are abundantly available (Pulkka *et al.*, 2014; Roy *et al.*, 2019). One of the promising methods for wastewater treatment to avoid toxic or dangerous materials is the photocatalytic degradation of dyes under solar and UV radiation (Rani *et al.*, 2018). Recently, metallic nanoparticles are widely used both in research and industry for photocatalytic degradation of MB removal from wastewater due to their high adsorption capacity, and less diffusion resistance with large surface area (Moradi *et al.*, 2018; Jabbari and Ghasemi, 2021). Among these metallic nanoparticles, AgNPs are well-known as an effective photocatalytic agent for the degradation of organic contaminants such as MB in water when exposed to UV light and sunlight irradiation due to either large surface area or quantum confinement effects of charge carriers. In a photocatalytic system, photo-induced reactions first occur at

the catalyst's surface. Then, the chemical constituents of plant extracts are one of the factors that affect the photodegradation capability of MB. In addition, AgNPs exhibited antifungal and antibacterial activities that improve the efficiency of wastewater treatment (Mohammadia *et al.*, 2020; Vanaja *et al.*, 2014, Rajkumar *et al.*, 2021). Hence, the research to find suitable plant varieties for extracts-based green synthesis of AgNPs for application in the photodegradation of MB is a matter of increasing interest.

In this research, a novel green, simple and environmental-friendly synthesis of AgNPs using *D. longifolia* extract and evaluating their photocatalytic degradation efficiency of MB in an aqueous solution under sunlight radiation is reported. Moreover, the effects of plant extract amount, AgNO<sub>3</sub> concentration, temperature, and time of reaction of AgNPs synthesis have also been performed.

## Materials and Methods

*D. longifolia* plants were collected in Son La province, Viet Nam. Analytical grades of AgNO<sub>3</sub> (99.8%), and MB were purchased from Merck chemicals without further purification.

### Preparation of *D. Longifolia* Extracts

*D. longifolia* plants were thoroughly washed with deionized water, then dried at 50°C, and crushed with a grinder to change into powder form. The powders were extracted with deionized water. The obtained aqueous extract was evaporated in a vacuum to afford an aqueous extract. The extract was then subjected to phytochemical analysis to detect the chemical constituents present in the extract.

100 mL of deionized water was added to 10 g of dried powder. The mixture was ultrasound extracted for 60 min before being filtered by Whatman filter No.1 paper. The filtrate obtained was used at 4°C for the biosynthesis of AgNPs.

### Qualitative Phytochemical Tests of Plant Extract

The chemical constituents of *D. longifolia* aqueous extract were qualitatively tested using standard methods such as alkaloids with Mayer's, Wagner's, Hager's, and Dragendorff's reagents; glycosides using Modified Brontragers test; steroids with Salkowski's test; phenolic compounds using ferric chloride test; flavonoids with lead acetate test and zinc hydrochloric acid reduction test; triterpenoids with copper acetate test and Noller's test. They were identified using standard procedures by characteristic color changes and precipitation reactions (Pandey and Tripathi, 2014; Yadav *et al.*, 2014).

### Synthesis of AgNPs

The *D. longifolia* extract above was added to 10 mL of AgNO<sub>3</sub> solution and stirred at 800 rpm. Then, NaOH 0.1 N was used to adjust the pH of the reaction mixture. The mixture was stirred continuously. The color of the reaction mixture changed from yellowish to dark yellow and then to brown at the end of the reaction. The AgNPs were obtained by centrifuging at 13000 rpm for 10 min to remove the impurities and subsequently dispersed in deionized water and used for further characterization.

### Characterization of AgNPs

Characteristics of the AgNPs were investigated using various techniques such as UV-Vis spectroscopy (UH5300, Hitachi, Japan), FTIR spectra (Perkin Elmer Spectrum Two), and SEM (Hitachi S-4800), XRD (D2-Phaser, Bruker, Japan). Debye-Scherrer Eq. (1) was used to calculate the crystallite size:

$$D = \frac{k\lambda}{\beta \cos \theta} \quad (1)$$

where, *D* is the particle size (nm),  $\lambda$  is the X-ray wavelength ( $\lambda = 0.15406$  nm), *k* is the Scherrer constant (*k* = 0.9),  $\lambda$  is the full width at half maximum (radians),  $\theta$  is the angle of diffraction (radians).

### Photocatalytic Degradation of MB

The photocatalytic capability of the AgNPs was determined by carrying out the MB degradation in the presence of sunlight. AgNPs were dispersed in 100 mL MB solution for 10 min using ultrasonication. The obtained solution was adjusted to pH = 6 and stirred in the dark for 30 min to achieve an adsorption equilibrium. Then, the solution was exposed to sunlight and centrifuged for 10 min at 13000 rpm. The MB degradation rate was identified by absorbance at 664 nm using a UV-Vis spectrophotometer. The efficiency of photocatalytic degradation was determined by Eq. (2):

$$\text{Degradation}(\%) = \frac{A_0 - A}{A_0} \times 100 \quad (2)$$

where, *A*<sub>0</sub> represents MB's initial absorbance and *A* is MB's absorbance after degradation. Moreover, the photodegradation rate was determined by calculating the rate constant, *k* (min<sup>-1</sup>), based on the pseudo-first-order reaction kinetics curves, as shown in Eq. (3) (Hasija *et al.*, 2019):

$$\ln\left(\frac{C_0}{C}\right) = kt \quad (3)$$

where, *C*<sub>0</sub> and *C* are the concentration of MB at initial and *t* time, respectively and *k* is the rate constant and calculated from the graph between ln(*C*/*C*<sub>0</sub>) verse irradiation time.

## Results

### Phytochemical Screening

The results of the phytochemical analysis of the *D. longifolia* extract are shown in Table 1 of the Supplementary material.

### Synthesis and Characteristics of AgNPs

The plant extract amount, AgNO<sub>3</sub> concentration, reaction temperature, and time are the main factors that impact the yields of formation and quality of nanoparticles. Hence, to produce nanoparticles of the desired morphology and size, these factors were optimized. Figure 1 displays the UV-Vis spectra of synthesized AgNPs at the different amounts of extract, temperatures, times, and absorption intensity versus reaction time.

The properties of AgNPs are characterized by FT-IR, XRD, and SEM analyses. The results of the characteristics of biosynthesized AgNPs are shown in Fig. 2.

### Photocatalytic Degradation of MB Dye

The mechanism of photocatalytic degradation of MB under solar light using synthesized AgNPs is illustrated in Fig. 3.

**Table 1:** Comparison of the MB degradation of biosynthesized AgNPs with previous reports

Biosynthesized AgNPs	Light source	Dose of catalyst (mg)	Dose of MB	Degradation time (min)	Degradation percentage (%)	Ref.
<i>Crataegus pentagyna</i> –AgNPs	Sunlight	30	15 mL, 0.06 mM	90	78.00	Ebrahimzadeh <i>et al.</i> (2020)
<i>Morinda tinctoria</i> -AgNPs	Sunlight	10	100 mL, 10 mg/L	4320	95.00	Vanaja <i>et al.</i> (2014)
<i>Jasminum</i> -AgNPs	Sunlight	10	100 mL	120	72.00	Aravind <i>et al.</i> (2021)
<i>Cauliflower</i> -AgNPs	Sunlight	5	50 mL, 1.00 mg/L	150	97.57	Kadam <i>et al.</i> (2020)
<i>D. longifolia</i> -AgNPs	Sunlight	20	100 mL, 5.00 mg/L	240	100.00	This study

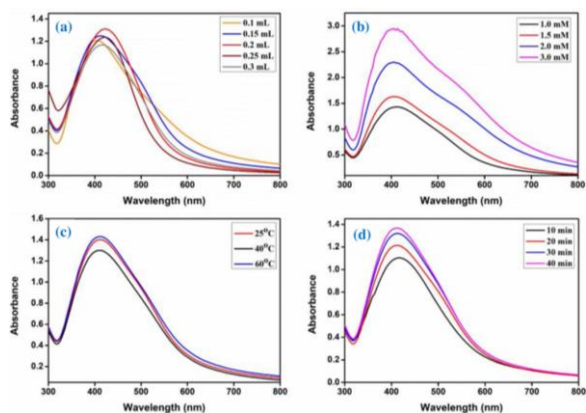


**Fig. 1:** UV-Vis spectra of synthesized AgNPs: (a) At the different amounts of extract; (b) At different temperatures; (c) At different times; (d) The absorption intensity versus reaction time

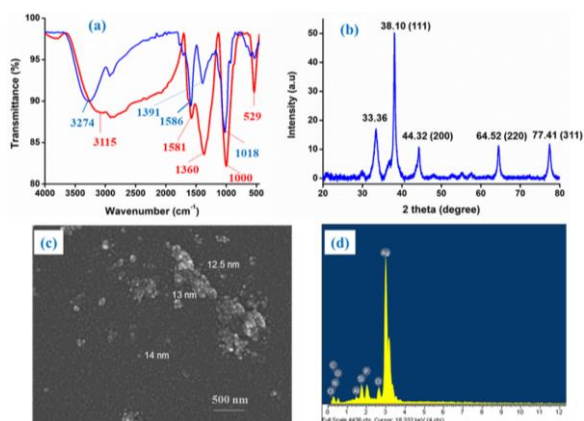


**Fig. 2 (a):** FT-IR spectra of the extract and AgNPs; (b) XRD pattern; (c) SEM image; (d) EDX spectra of AgNPs

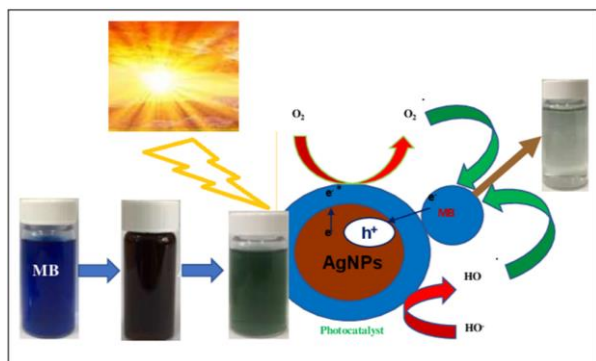


**Fig. 3:** Proposed mechanism of photocatalytic degradation of MB by AgNPs under solar light

Figure 4 shows the effect of different irradiation times, photocatalyst's dose, and initial dye concentration on MB photodegradation using the biosynthesized AgNPs and kinetic curves,  $\ln(C_0/C)$  versus time of AgNPs for MB degradation.

## Discussion

### Phytochemical Screening

The aqueous extract of *D. longifolia* exhibited the existence of flavonoids, steroids, triterpenoids, phenolic compounds, and glycosides, while alkaloids were absent (Table 1 of Supplementary material). These compounds are known to be reducing, capping, and stabilizing agents for synthesizing AgNPs. Therefore, the synthesis of AgNPs can be performed using the aqueous extract of *D. longifolia*.

### Synthesis of AgNPs

#### Effect of Extract Amount

The amount variation study of the extract was carried out with the amount of extract (0.1 to 0.3 mL). Figure 1a shows the UV-Vis spectroscopy of biosynthesized AgNPs with different volumes of extract. It was found that as the volumes of extract increased from 0.1 to 0.2 mL, the absorption intensity increased gradually and the absorption peak shifted from 404 to 422 nm, respectively. However, with higher extracts amounts (0.25 and 0.3 mL), the absorption intensity decreased and the absorption peak shifted from 422 to 416 nm. This decrease could be ascribed to the completely excess extract left in the solution after forming AgNPs. Based on these results, 0.2 mL of *D. longifolia* extract was considered the optimal amount for producing AgNPs.

#### Effect of AgNO<sub>3</sub> Concentration

AgNPs were synthesized at different concentrations of AgNO<sub>3</sub> (1-3 mM using 0.2 mL extract). Figure 1b presents an increasing broadness of absorption peak at the range of wavelength from 400 to 420 nm when the concentration of the AgNO<sub>3</sub> is up to 3 mM. This result was attributed that at the high concentration of AgNO<sub>3</sub>, the additional interaction between secondary reduction and the surface stabilizing molecules occurred on the surface of preformed nuclei.

This result indicates that the concentration of 1.5 mM was suitable for synthesizing AgNPs using *D. longifolia*.

#### Effect of Reaction Temperature

The effect of different temperatures (25-40°C) was also evaluated for *D. longifolia* extract-mediated AgNPs synthesis as seen in Fig. 1c. when the temperature increases from 25 to 40°C, the absorption intensity is raised. A minor increase in the absorption intensity when the temperature reaches 60°C-the stable and undecomposed of most organic compound's temperature. We selected 40°C as the most suitable temperature for the synthesis of AgNPs.

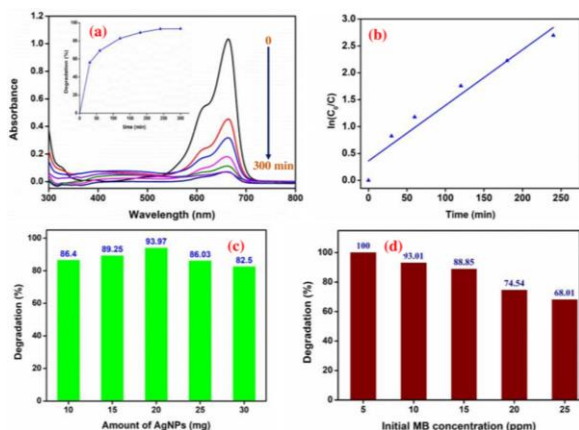


**Fig. 4 (a):** Uv-Vis spectra of MB solution under sunlight irradiation with the presence of AgNPs with different irradiation times; (b) kinetic curves,  $\ln(C_0/C)$  versus time of AgNPs for MB degradation under simulated solar light irradiation; (c) effect of photocatalyst's

### Effect of Reaction Time

To optimize the reaction time, the time variation study used the designated concentration of  $\text{AgNO}_3$  (2 mm) and extract amount (0.2 mL) to optimize the reaction time. The UV-Vis spectra of AgNPs produced at different time durations are shown in Fig. 1d. The absorption intensity of the 414 nm SPR band increased as the reaction time progressed, and after 40 min, the absorption intensity slightly increased. Therefore, 30 min was selected to synthesize AgNPs.

### Characteristics of AgNPs

#### FT-IR Spectroscopy

FTIR is a useful tool for determining the organic functional groups present in the extracts of plants and observing the possible interaction of biomolecules with the AgNPs surfaces. The FT-IR spectra of *D. longifolia* extract (Fig. 2a) reveal the characteristic absorption bands at 3274, 1586, 1391, and 1018  $\text{cm}^{-1}$  which were shifted to 3115, 1581, 1360, and 1000  $\text{cm}^{-1}$  in the FT-IR of AgNPs  $\text{cm}^{-1}$ , respectively. The presence of these groups in the FTIR spectra indicated that the plant extract and AgNPs contained a significant number of polyphenols and saponins. In addition, the FTIR spectra of AgNPs appeared at the absorption peak at a wavenumber of 529  $\text{cm}^{-1}$ , which is typical for the vibration of Ag-organic functional groups.

#### XRD Analysis

XRD study was used to understand the phase structure and crystalline nature of AgNPs. In the XRD pattern of AgNPs, as shown in Fig. 2b, Bragg's

reflection was observed at  $2\theta$  values of 38.10, 44.32, 64.52, and 77.41, representing the planes of (111), (200), (220), and (311) which related to the face-centered cubic crystalline structure of AgNPs. Moreover, the appearance of the small peak at 33.36 was assigned to the crystalline organic constituents. These results agree with the previous reports (Wei *et al.*, 2020). The average crystallite size of synthesized AgNPs is estimated to be around 13 nm using Eq. 1.

### SEM Analysis

SEM image was used to evaluate the distributions and surface morphology of AgNPs. The AgNPs were mostly aggregated into nanoclusters, as presented in Fig. 2c. In addition, the AgNPs were generally spherical with an average particle size of 13~14 nm. This result is in good agreement with the value determined by the analysis of XRD. However, the morphology of the AgNPs was poorly defined and irregular because of the different reduction ways in which silver ions can take in a complex solution consisting of reducing agents such as flavonoids, terpenoids, and alkaloids de Barros Santos *et al.*, 2015). Moreover, the Dispersive-Energy X-ray (EDX) spectra of AgNPs were performed to analyze the elementary distribution, as shown in Fig. 2d. The elemental signals of silver atoms in the AgNPs sample are homogeneously found at 3 keV. The results show that other elements such as nitrogen, chlorine, and carbon exist in the sample of *D. longifolia* extracts

### Photocatalytic Degradation of MB Dye

The dominant mechanism of the degradation of hazardous organic dyes is photocatalysis. Upon irradiation, electrons move from the valence band to the conduction band when excited, resulting in the formation of electron-hole pairs on the surface of the photocatalyst (Marimuthu *et al.*, 2020). AgNPs have a large surface area with high pores so they are an active source for the photodegradation of MB dye under sunlight (Wang *et al.*, 2012). As shown in Fig. 3, when silver nanoparticles absorb UV irradiation of sunlight, electrons from the 4d orbital are excited to the 5sp orbital, resulting in many exciting photogenerated electrons. Then, these electrons transfer the oxygen molecules and hydroxyl ions into oxygen radicals ( $\text{O}_2\cdot$ ) and Hydroxyl radicals ( $\text{HO}\cdot$ ), respectively. These radicals oxidize MB dye and generate holes in the d orbital of nanoparticles. The formed holes gain the electrons from dye molecules that adsorbed on the surface of nanoparticles, causing further MB degradation. As a result of the SPR effect and the interband transition, AgNPs are known to absorb UV light (Singh and Dhaliwal, 2018). Solar light-mediated photocatalytic degradation of MB by AgNPs depends on factors such as the dye concentration, degradation time, and the amount of catalyst. Thus, we investigated

the effect of these factors on factors on the photocatalytic degradation of MB using AgNPs as a catalyst.

#### *Effect of Contact Time*

Figure 4a presented the influence of time on removing MB using 20 mg of AgNPs. The result displayed that photocatalytic degradation of MB dye occurred. Firstly, when adding AgNPs to the MB solution, the color of the solution changed from deep blue to dark green. Then, when exposed to sunlight, the intensity of the dark green color decreased with increasing time. The efficiency of photocatalytic degradation was calculated using the change in absorbance at 665 nm. The MB degradation increased with contact time up to 240 min, from 240 to 300 min, the degradation was insignificant. Therefore, the highest percentage of the degradation of MB dye using AgNPs as a catalyst was 93.10% in 240 min.

Moreover, the obtained data fitted to the pseudo-first-order kinetic model perfectly, as shown in Fig. 4b with the R<sup>2</sup> value of 0.9505. By linear fitting  $\ln(C_0/C)$  against time, the photodegradation rate constant  $k$  was obtained at  $0.01034 \text{ min}^{-1}$ .

#### *Effect of Catalyst Dose*

The optimal catalyst dose must be calculated to avoid using too much catalyst. The effects of catalyst doses on the removal efficiency of MB were investigated by varying the doses from 10 to 30 mg at the same MB concentration of 10 mg/L. As shown in Fig. 4c, when the amount of the catalyst increased from 10 to 20 mg, the photodegradation rate rose, but photodegradation efficiency decreased as the catalyst dose increased from 25 to 30 mg. It is possible to explain that at higher catalyst doses, the activated molecules were deactivated by collision with ground-state catalysts, resulting in a lower reaction rate.

#### *Effect of Dye Concentration*

The effects of dye concentration on percentage degradation were studied under sunlight irradiation by varying the initial concentrations of MB from 5 to 25 ppm with optimum catalyst loading. Figure 4d showed that the removal percentage of dye decreased from 100 to 68.01% with increasing the initial concentrations of MB from 5 to 25 ppm after 240 min of irradiation. These results illustrate that at lower concentrations, MB molecules are adsorbed on the surface of silver nanoparticles at more active sites so the degradation efficiency is higher. In contrast, as the initial concentration of MB is raised, the MB molecules adsorbed light and the photons never reached. As a result, the photodegradation of MB using biosynthesized AgNPs decreased. Thus, the removal efficiency of MB dye was found to be better at low dye concentrations.

Table 1 compares the MB degradation of biosynthesized AgNPs with previous reports. The biosynthesized AgNPs exhibited greater photocatalytic efficiency under solar light than similar catalysts. This result may be explained that the phytochemicals present in the *D. longifolia* extract, such as spirostan, and furostan saponins (Fig. 1 of Supplementary material) and even in the nanoparticle surface not only prevent the aggregation of nanoparticles during MB degradation but also improve the absorption of UV light and inhibits the recombination of photogenerated electrons and holes in the process of photodegradation. As a result, the photodegradation of MB using biosynthesized AgNPs was more effective.

## Conclusion

In summary, AgNPs have been successfully synthesized via a simple one-pot method using *D. longifolia* extract. The 0.2 mL of *D. longifolia* extract, 1.5 mM AgNO<sub>3</sub> concentration, 40°C, and 30 min were optimal conditions for producing the desired AgNPs. The results of the SEM image confirmed that the nanoparticles were generally spherical and their average size was around 13~14 nm. In particular, a simple mechanism of the photocatalytic reaction was elucidated by the generated electron-hole pairs on the nanoparticle surface. The great photocatalytic ability with the 100% degradation yield of biosynthesized AgNPs was achieved after 240 min illumination. The chemical constituents of *D. longifolia* extract contributed significantly to the degradation efficiency of AgNPs. The results of MB degradation indicated that *D. longifolia* extract-mediated AgNPs can have significant photocatalytic activity when exposed to sunlight. AgNPs can be a suitable candidate for organic dye removal such as MB, which poses serious environmental risks.

## Acknowledgment

Author thanks TNU-University of Sciences in Vietnam.

## Funding Information

This research was funded by TNU-University of Sciences in Vietnam with grant number CS2020-TN06-12.

## Author's Contributions

**Khieu Thi Tam:** Conceptualization, methodology, formal analysis, resources, software, visualization, writing-original draw.

**Dang Van Thanh and Huu Tap Van:** Formal analysis, methodology.

**Nguyen Thi Phuong Mai and Cao Thanh Hai:**  
Formal analysis.

**Tran Minh Phuong and Nguyen Thi Xuan:**  
Conceptualization, data curation.

**Van-Truong Nguyen:** Resources, supervision, visualization, writing-review and edited.

## Ethics

This article is original and all data has been published. All authors have read and approved the manuscript. No ethical problems are contained.

## References

- Aravind, M., Ahmad, A., Ahmad, I., Amalanathan, M., Naseem, K., Mary, S. M. M., ... & Zuber, M. (2021). Critical green routing synthesis of silver NPs using jasmine flower extract for biological activities and photocatalytic degradation of methylene blue. *Journal of Environmental Chemical Engineering*, 9(1), 104877. <https://doi.org/10.1016/j.jece.2020.104877>
- Bera, A., & Belhaj, H. (2016). Application of nanotechnology employing nanoparticles and nanodispersions in oil recovery-A comprehensive review. *Journal of Natural Gas Science and Engineering*, 34, 1284-1309. <https://doi.org/10.1016/j.jngse.2016.08.023>
- Bich, D. H., Chung, D. Q., Chuong, B. X., Dong, N. T., Dam, D. T., Hien, P. V., ... & Toan, T. (2004). The medicinal plants and animals in Vietnam. *Hanoi Science and Technology Publishing House, Hanoi*, 1, 224.
- Chi, V. V. (2012). Dictionary of medicinal plants in Vietnam. *Medical Publishing House, Hanoi*, 1, 441-442.
- de Barros Santos, E., Madalossi, N. V., Sigoli, F. A., & Mazali, I. O. (2015). Silver nanoparticles: Green synthesis, self-assembled nanostructures and their application as SERS substrates. *New Journal of Chemistry*, 39(4), 2839-2846. <https://doi.org/10.1039/C4NJ02239D>
- Ebrahimzadeh, M. A., Naghizadeh, A., Amiri, O., Shirzadi-Ahodashti, M., & Mortazavi-Derazkola, S. (2020). Green and facile synthesis of Ag nanoparticles using Crataegus pentagyna fruit extract (CP-AgNPs) for organic pollution dyes degradation and antibacterial application. *Bioorganic Chemistry*, 94, 103425. <https://doi.org/10.1016/j.bioorg.2019.103425>
- Gour, A., & Jain, N. K. (2019). Advances in green synthesis of nanoparticles. *Artificial Cells, Nanomedicine, and Biotechnology*, 47(1), 844-851. <https://doi.org/10.1080/21691401.2019.1577878>
- Hasija, V., Sudhaik, A., Raizada, P., Hosseini-Bandegharai, A., & Singh, P. (2019). Carbon quantum dots supported AgI/ZnO/phosphorus doped graphitic carbon nitride as Z-scheme photocatalyst for efficient photodegradation of 2, 4-dinitrophenol. *Journal of Environmental Chemical Engineering*, 7(4), 103272. <https://doi.org/10.1016/j.jece.2019.103272>
- Hong, X., Wen, J., Xiong, X., & Hu, Y. (2016). Shape effect on the antibacterial activity of silver nanoparticles synthesized via a microwave-assisted method. *Environmental Science and Pollution Research*, 23(5), 4489-4497. <https://doi.org/10.1007/s11356-015-5668-z>
- Houas, A., Lachheb, H., Ksibi, M., Elaloui, E., Guillard, C., & Herrmann, J. M. (2001). Photocatalytic degradation pathway of methylene blue in water. *Applied Catalysis B: Environmental*, 31(2), 145-157. [https://doi.org/10.1016/S0926-3373\(00\)00276-9](https://doi.org/10.1016/S0926-3373(00)00276-9)
- Hussain, I., Singh, N. B., Singh, A., Singh, H., & Singh, S. C. (2016). Green synthesis of nanoparticles and its potential application. *Biotechnology Letters*, 38(4), 545-560. <https://doi.org/10.1007/s10529-015-2026-7>
- Ishak, N. M., Kamarudin, S. K., & Timmiati, S. N. (2019). Green synthesis of metal and metal oxide nanoparticles via plant extracts: An overview. *Materials Research Express*, 6 (11), 112004.
- Jabbari, R., & Ghasemi, N. (2021). Investigating methylene blue dye adsorption isotherms using silver nano particles provided by aqueous extract of tragopogon buphthalmoides. *Chemical Methodologies*, 5(1), 21-29. <http://chemmethod.com>
- Kadam, J., Dhawal, P., Barve, S., & Kakodkar, S. (2020). Green synthesis of silver nanoparticles using cauliflower waste and their multifaceted applications in photocatalytic degradation of methylene blue dye and Hg<sup>2+</sup> biosensing. *SN Applied Sciences*, 2(4), 1-16. <https://doi.org/10.1007/s42452-020-2543-4>
- Khatri, A., Peerzada, M. H., Mohsin, M., & White, M. (2015). A review on developments in dyeing cotton fabrics with reactive dyes for reducing effluent pollution. *Journal of Cleaner Production*, 87, 50-57. <https://doi.org/10.1016/j.jclepro.2014.09.017>
- Kuntyi, O., Mazur, A., Kytsya, A., Karpenko, O., Bazylyak, L., Mertsalo, I., ... & Prokopalo, A. (2020). Electrochemical synthesis of silver nanoparticles in solutions of rhamnolipid. *Micro & Nano Letters*, 15(12), 802-807. <https://doi.org/10.1049/mnl.2020.0195>
- Maharjan, S., Liao, K. S., Wang, A. J., Zhu, Z., McElhenny, B. P., Bao, J., & Curran, S. A. (2020). Sol-gel synthesis of stabilized silver nanoparticles in an organosiloxane matrix and its optical nonlinearity. *Chemical Physics*, 532, 110610. <https://doi.org/10.1016/j.chemphys.2019.110610>

- Marimuthu, S., Antonisamy, A. J., Malayandi, S., Rajendran, K., Tsai, P. C., Pugazhendhi, A., & Ponnusamy, V. K. (2020). Silver nanoparticles in dye effluent treatment: A review on synthesis, treatment methods, mechanisms, photocatalytic degradation, toxic effects and mitigation of toxicity. *Journal of Photochemistry and Photobiology B: Biology*, 205, 111823.  
<https://doi.org/10.1016/j.jphotobiol.2020.111823>
- Mehdizadeh, S., Ghasemi, N., Ramezani, M., & Mahanpoor, K. (2021). Biosynthesis of Silver Nanoparticles Using Malva Sylvestris Flower Extract and Its Antibacterial and Catalytic Activity. *Chemical Methodologies*, 5(4), 356-366.
- Mohammadlinejad, S., Almasi, H., & Esmaili, M. (2019). Simultaneous green synthesis and in-situ impregnation of silver nanoparticles into organic nanofibers by *Lythrum salicaria* extract: Morphological, thermal, antimicrobial and release properties. *Materials Science and Engineering: C*, 105, 110115.  
<https://doi.org/10.1016/j.msec.2019.110115>
- Mohammadi, S. S., N. Ghasemi, M. Ramezani and S. Khaghani (2021) "Biosynthesis of silver nanoparticles using the *Falcaria Vulgaris (Alisma Plantago-Aquatica L.)* extract and optimum synthesis." *Chemical Methodologies* 5(4), 296-307.
- Mohammadia, S. S., N. Ghasemia and M. Ramezania (2020) "Bio-fabrication of silver nanoparticles using naturally available wild herbaceous plant and its antibacterial activity". *Eurasian Chemical Communications*, 87-102.
- Moradi, S., Taghavi Fardood, S., & Ramazani, A. (2018). Green synthesis and characterization of magnetic NiFe<sub>2</sub>O<sub>4</sub>@ ZnO nanocomposite and its application for photocatalytic degradation of organic dyes. *Journal of Materials Science: Materials in Electronics*, 29(16), 14151-14160.  
<https://doi.org/10.1007/s10854-018-9548-4>
- Nguyen, A. T., Fontaine, J., Malonne, H., & Duez, P. (2006). Homoisoflavanones from *Disporopsis aspera*. *Phytochemistry*, 67(19), 2159-2163.  
<https://doi.org/10.1016/j.phytochem.2006.06.021>
- Pandey, A., & Tripathi, S. (2014). Concept of standardization, extraction and pre phytochemical screening strategies for herbal drug. *Journal of Pharmacognosy and Phytochemistry*, 2(5).
- Piszczyk, P., & Radtke, A. (2018). Silver nanoparticles fabricated using chemical vapor deposition and atomic layer deposition techniques: Properties, applications and perspectives: Review. *Noble and Precious Metals; Seehra, MS, Bristow, AD, Eds*, 187-213.
- Pulkka, S., Martikainen, M., Bhatnagar, A., & Sillanpää, M. (2014). Electrochemical methods for the removal of anionic contaminants from water—a review. *Separation and Purification Technology*, 132, 252-271.  
<https://doi.org/10.1016/j.seppur.2014.05.021>
- Rafique, M., Sadaf, I., Rafique, M. S., & Tahir, M. B. (2017). A review on green synthesis of silver nanoparticles and their applications. *Artificial Cells, Nanomedicine, and Biotechnology*, 45(7), 1272-1291.  
<https://doi.org/10.1080/21691401.2016.1241792>
- Rajkumar, R., Ezhumalai, G., & Gnanadesigan, M. (2021). A green approach for the synthesis of silver nanoparticles by *Chlorella vulgaris* and its application in photocatalytic dye degradation activity. *Environmental Technology & Innovation*, 21, 101282.  
<https://doi.org/10.1016/j.eti.2020.101282>
- Rani, B., Punniyakoti, S., & Sahu, N. K. (2018). Polyol asserted hydrothermal synthesis of SnO<sub>2</sub> nanoparticles for the fast adsorption and photocatalytic degradation of methylene blue cationic dye. *New Journal of Chemistry*, 42(2), 943-954.
- Roy, A., Bulut, O., Some, S., Mandal, A. K., & Yilmaz, M. D. (2019). Green synthesis of silver nanoparticles: Biomolecule-nanoparticle organizations targeting antimicrobial activity. *RSC advances*, 9(5), 2673-2702. <https://doi.org/10.1039/C8RA08982E>
- Saini, R. D. (2017). Textile organic dyes: Polluting effects and elimination methods from textile waste water. *Int J Chem Eng Res*, 9(1), 121-136.  
<http://www.ripublication.com>
- Salem, S. S., & Fouda, A. (2021). Green synthesis of metallic nanoparticles and their prospective biotechnological applications: An overview. *Biological Trace Element Research*, 199(1), 344-370.  
<https://doi.org/10.1007/s12011-020-02138-3>
- Singh, J., & Dhaliwal, A. S. (2018). Plasmon-induced photocatalytic degradation of methylene blue dye using biosynthesized silver nanoparticles as photocatalyst. *Environmental Technology*.  
<https://doi.org/10.1080/09593330.2018.1540663>
- Tan, K. A., Morad, N., & Ooi, J. Q. (2016). Phytoremediation of methylene blue and methyl orange using *Eichhornia crassipes*. *International Journal of Environmental Science and Development*, 7(10), 724.  
<https://doi.org/10.18178/ijesd.2016.7.10.869>
- Thu Ha, T. T., Vui, D. K., Hoang, N. H., Tai, B. H., & Van Kiem, P. (2021). Dispolongiosides A and B, Two New Fucose Containing Spirostanol Glycosides from the Rhizomes of *Disporopsis longifolia* Craib., and Their Nitric Oxide Production Inhibitory Activities. *Natural Product Communications*, 16(10), 1934578X211055013.  
<https://doi.org/10.1177/1934578X211055>



- Vanaja, M., Paulkumar, K., Baburaja, M., Rajeshkumar, S., Gnanajobitha, G., Malarkodi, C., ... & Annadurai, G. (2014). Degradation of methylene blue using biologically synthesized silver nanoparticles. *Bioinorganic Chemistry and Applications*, 2014. <https://doi.org/10.1155/2014/742346>
- Vanlalveni, C., Lallianrawna, S., Biswas, A., Selvaraj, M., Changmai, B., & Rokhum, S. L. (2021). Green synthesis of silver nanoparticles using plant extracts and their antimicrobial activities: A review of recent literature. *RSC Advances*, 11(5), 2804-2837. <https://doi.org/10.1039/D0RA09941D>
- Wang, G., & Nie, F. T. (2010). Chemical constituents from *Disporopsis pernyi*. *Chin Tradit Pat Med*, 11, 1936-1938.
- Wang, P., Huang, B., Dai, Y., & Whangbo, M. H. (2012). Plasmonic photocatalysts: Harvesting visible light with noble metal nanoparticles. *Physical Chemistry Chemical Physics*, 14(28), 9813-9825. <https://doi.org/10.1039/C2CP40823F>
- Wei, S., Wang, Y., Tang, Z., Hu, J., Su, R., Lin, J., ... & Xu, R. (2020). A size-controlled green synthesis of silver nanoparticles by using the berry extract of *Sea Buckthorn* and their biological activities. *New Journal of Chemistry*, 44(22), 9304-9312. <https://doi.org/10.1039/D0NJ01335H>
- Yadav, M., Chatterji, S., Gupta, S. K., & Watal, G. (2014). Preliminary phytochemical screening of six medicinal plants used in traditional medicine. *Int J Pharm Pharm Sci*, 6(5), 539-42.
- Yang, Q. X., Xu, M., Zhang, Y. J., Li, H. Z., & Yang, C. R. (2004). Steroidal saponins from *Disporopsis pernyi*. *Helvetica Chimica Acta*, 87(5), 1248-1253. <https://doi.org/10.1002/hlca.200490114>